

On near integrability of some impact systems

M. Pnueli¹, V. Rom-Kedar^{1,2}

¹ Department of Computer Science and Applied Mathematics,

The Weizmann Institute of Science, Rehovot, Israel

² The Estrin Family Chair of Computer Science and Applied Mathematics.

March 30, 2018

Abstract

A class of Hamiltonian impact systems exhibiting smooth near integrable behavior is presented. The underlying unperturbed model investigated is an integrable, separable, 2 degrees of freedom mechanical impact system with effectively bounded energy level sets and a single straight wall which preserves the separable structure. Singularities in the system appear either as trajectories with tangent impacts or as singularities in the underlying Hamiltonian structure (e.g. separatrices). It is shown that away from these singularities, a small perturbation from the integrable structure results in smooth near integrable behavior. Such a perturbation may occur from a small deformation or tilt of the wall which breaks the separability upon impact, the addition of a small regular perturbation to the system, or the combination of both. In some simple cases explicit formulae to the leading order term in the near integrable return map are derived. Near integrability is also shown to persist when the hard billiard boundary is replaced by a singular, smooth, steep potential, thus extending the near-integrability results beyond the scope of regular perturbations. These systems constitute an additional class of examples of near integrable impact systems, beyond the traditional one dimensional oscillating billiards, nearly elliptic billiards, and the near-integrable behavior near the boundary of convex smooth billiards with or without magnetic field.

1 Background

The global phase-space structure of smooth nonlinear n d.o.f. Hamiltonian systems with $n \geq 2$ is usually unknown. While numerical simulations for such systems are readily available, they are usually difficult to interpret due to our limited perception of high dimensional spaces. Moreover, the abundance of various phase space structures in such systems (tori, cantori, homoclinic tangencies,

lower dimensional whiskered tori etc.), shadowed by chaotic solutions, complicates the dynamics and its averaged and asymptotic expressions. One therefore seeks to study special classes of systems which are amenable to analysis in some limit and inspire the definition of particular observables and projections that detect the closeness of the given system to its limiting behavior. Traditional examples are near-integrable systems and slow-fast systems [1, 2, 15]. More recently, analytical tools for studying smooth near-billiard and near-impact systems have been developed [18, 30, 27, 20, 17]. In these works, the limit system is a Hamiltonian Impact System (HIS) which describes the dynamics of a particle moving under the influence of a potential inside a domain and reflecting elastically from its boundary. Billiards correspond to the simplest HIS with inertial motion (trivial potential) in the domain interior. By this approach, to better understand systems with very steep potentials at the domain's boundary, one studies the limit system in which the steep part is replaced by impacts. Once the dynamics under the HIS are known, one establishes which of its features persist [27, 17] and how those which do not persist bifurcate [30, 28].

The study of HIS combines the features of Hamiltonian dynamics and those of piecewise smooth dynamical systems [7, 19, 22], which are specific examples of hybrid systems (e.g. [16, 14]). Utilizing the Hamiltonian structure, one hopes to gain information on global scales. Yet, impacts destroy the smoothness [9, 18] and possibly the integrability of the underlying Hamiltonian flow [20]. Finding integrable HIS and studying their behavior under perturbations (of the boundary and of the potential) expands the families of non-linear systems which we can analyse and, by utilizing the smooth impact framework, allows to establish near-integrability results even though the perturbation terms in this case are formally large in the C^r topology. Here we provide such a class of prototype impact systems which are near-integrable and are amenable to analysis. Previous near-integrability results for HIS have utilized the local dynamics near periodic orbits [11, 4, 5, 17], near a smooth convex boundary [31, 6, 5] and near saddle-center homoclinic connection of a quadratic potential with impacts [20]. Another approach utilized the generalized adiabatic theory in 1.5 d.o.f. systems, where the Hamiltonian dynamics are in one dimension and the boundary is slowly oscillating [12, 13, 25, 3]. Similar approaches were employed in the study of magnetic billiards [29, 6, 4, 5].

Here we address the subject of global structure and stability of orbits on large portions of the phase space by identifying regimes in which standard smooth near-integrable results apply (in particular, persistence of KAM tori and the emergence of resonances). These objects arise even though, formally, we are far from the classical setup of smooth small perturbations to smooth integrable systems. To this aim, we focus on 2 degrees of freedom mechanical impact systems, where the underlying Hamiltonian is of the form $H = \frac{p_1^2}{2} + \frac{p_2^2}{2} + V(q_1, q_2)$ and $V(\cdot)$ is a separable, smooth (C^{r+1}) potential with effectively bounded level sets. The impact in the system is realized as a single straight vertical wall, where the separability assumption is with respect to the vertical

wall coordinate system, so that this wall does not destroy integrability. A perturbation from the integrable structure is then realized by either the addition of a small, $\mathcal{O}(\epsilon_r)$, C^{r+1} regular coupling perturbation to the potential or a small $\mathcal{O}(\epsilon_w)$, C^{r+1} deformation of the wall. The main result here is that under some specific conditions, in a large ($\mathcal{O}(1)$ measure) phase space region, smooth near-integrable dynamics are realized for sufficiently small ϵ_r and ϵ_w . Moreover, using [17], it is shown that these results may be extended for the smooth system in which the hard wall is replaced by a soft steep potential, provided the potential is sufficiently steep (notably, the steeper the potential is the larger the perturbation is in the C^{r+1} topology).

The paper is organized as follows. In section 2, the underlying integrable structure of the systems investigated is presented, and an integrable Poincaré return map is constructed. Conditions for smoothness of the return map are shown, as well as the conditions for twist and for resonance. In Section 3, it is shown how, following the conclusions of section 2, one can achieve near integrability results when adding a small regular perturbation to the system or when considering a small deformation of the wall from the vertical, perpendicular position. Furthermore, it is shown that for the case of straight walls explicit formulae for the leading order terms of this return map in the wall inclination and the smooth perturbation term may be calculated as Melnikov-type integrals. Near integrability is also extended to the corresponding soft impact systems. An example to the main results is given in section 4, where, additionally, the global perturbed phase-space structure is presented in an impact-energy-momentum diagram. We summarize our results in section 5.

2 Setup and integrability results

Consider a 2 degrees of freedom mechanical impact system of the form:

$$H = H(\cdot; \epsilon_r, \epsilon_w, q^w, b) = H_{int}(q_1, p_1, q_2, p_2) + \epsilon_r V_r(q_1, q_2) + b \cdot V_b(q - q^w; \epsilon_w) \quad (1)$$

where the underlying integrable structure is separable (see below), the potential $V_r(q_1, q_2)$ corresponds to a regular smooth (C^{r+1} with $r > 3$) coupling term and the singular billiard potential $V_b(q - q^w; \epsilon_w)$ represents the singular impact term. Hereafter, for $\epsilon_w = 0$, the impact corresponds to a single vertical wall passing through the origin (namely, with no loss of generality, the q_2 axis is set along the wall and the origin is set at some point on the wall, otherwise shift the q_2 coordinate by a constant value). A non-zero ϵ_w corresponds to small perturbations, in C^{r+1} , from the vertical geometry, so $q^w = (q_1^w = \epsilon_w Q^w(q_2^w; \epsilon_w), q_2^w)$, and Q^w is a C^{r+1} function satisfying $Q^w(0; 0) = 0$. Motion occurs to the right of the wall; the wall is realized in the system as a singular energy

barrier:

$$V_b = \begin{cases} 0, & (q_1, q_2) : q_1 > \epsilon_w Q^w(q_2; \epsilon_w) \\ 1, & (q_1, q_2) : q_1 \leq \epsilon_w Q^w(q_2; \epsilon_w) \end{cases} \quad (2)$$

and b is either a fixed large number or zero (when positive it is taken such that for all energies of interest the wall is impassable, whereas $b = 0$ refers to the smooth Hamiltonian system without the impact).

The integrable structure of H_{int} of (1) is of the form:

$$H_{int} = \frac{\|p\|^2}{2} + V_{int}(q_1, q_2) = \frac{p_1^2}{2} + V_1(q_1) + \frac{p_2^2}{2} + V_2(q_2) = H_1(q_1, p_1) + H_2(q_2, p_2), \quad (3)$$

where the potential $V_{int} = V_1(q_1) + V_2(q_2)$ is Separable, C^{r+1} ($r > 3$) Smooth, Simple (has finite, discrete number of simple extremum points), Bounded from below and V_i go to infinity as $|q_i| \rightarrow \infty$, so H_{int} has only bounded level sets. Therefore the perturbation terms $V_r(\cdot), Q^w(\cdot)$ are bounded on the energy surfaces (see appendix), where the bound depends on H . Hereafter we assume that $H = \mathcal{O}(1)$ - the asymptotic behavior at large H may require additional analysis.

Definition 2.1. Integrable Hamiltonians of the form (3) satisfying the above conditions will hereafter be called *Hamiltonians of the S3B (Separable, Smooth, Simple, Bounded level sets) class*.

Next we define the phase space region for which the results apply. We first describe the smooth integrable structure. Denote, in each sub phase space $i = 1, 2$, the n_{ic} center fixed points by $(q_{ic, 1 \dots n_{ic}}, 0)$ and the n_{is} saddle fixed points by $(q_{is, 1 \dots n_{is}}, 0)$. Let $\mathbb{I}_{H_i}(H)$ denote the set of allowed H_i values for a given H (here, the interval $H_i \in [\min V_i, H - \min V_{\bar{i}}]$, where \bar{i} denotes the complement phase space to i), and let $\mathcal{N}_\delta(H_i^*)$ denote the δ - open interval of H_i values around H_i^* . The closed set of regular integrable H_i values on a given energy level H

$$\mathbb{H}_i^{R, \delta}(H) = \mathbb{I}_{H_i}(H) \setminus \left[\bigcup_{j=1}^{n_{is}} \mathcal{N}_\delta(H_i(q_{is, j}, 0)) \cup \bigcup_{j=1}^{n_{\bar{i}s}} \mathcal{N}_\delta(H - H_{\bar{i}}(q_{\bar{i}s, j}, 0)) \right], \quad \delta > 0, i = 1, 2 \quad (4)$$

corresponds to H_i values for which the Liouville leaves are bounded away from singularities, namely the energy of the level sets in both the (q_i, p_i) plane and in the $(q_{\bar{i}}, p_{\bar{i}})$ plane are at least δ - away from the energies of the planar singular level sets of the saddle points $q_{is}, q_{\bar{i}s}$ respectively (hereafter, normally elliptic lower dimensional tori are included in the regular set). Clearly, the measure of these H_i intervals is of $\mathcal{O}(1)$ when $\delta \rightarrow 0$:

$$|\mathbb{H}_i^{R, \delta}(H)| \geq H - \min V_i - \min V_{\bar{i}} - 2\delta(n_{is} + n_{\bar{i}s}). \quad (5)$$

Using the local action-angle variables for the smooth unperturbed integrable system ($\epsilon_r = 0, b = 0$), for all $H_2 \in \mathbb{H}_2^{R, \delta}(H)$, H_{int} can be written as $H_{int}(J, I) = H_1(J) + H_2(I)$, and the dynamics on

the corresponding leaves of the level sets are described by:

$$\begin{cases} \dot{\varphi} = \frac{\partial H_{int}}{\partial J} = \omega_1(J), & \dot{J} = -\frac{\partial H_{int}}{\partial \varphi} = 0 \\ \dot{\theta} = \frac{\partial H_{int}}{\partial I} = \omega_2(I), & \dot{I} = -\frac{\partial H_{int}}{\partial \theta} = 0 \end{cases} \Rightarrow \begin{cases} \varphi(t) = \varphi_0 + \omega_1(J_0) \cdot t & J(t) = J_0 \\ \theta(t) = \theta_0 + \omega_2(I_0) \cdot t & I(t) = I_0 \end{cases} \quad (6)$$

where $(J_0, \varphi_0) = S_1(q_1(0), p_1(0))$, $(I_0, \theta_0) = S_2(q_2(0), p_2(0))$ and S_i denote local transformations to action-angle coordinates on each leaf. A branch of the Liouville foliation corresponds to a family of regular leaves (here each leaf is a torus, each branch a one parameter family of tori). On each branch, away from the branch boundaries, the transformation to action-angle coordinates is smooth and well defined. For each H , the set $\mathbb{H}_2^{R,\delta}(H)$ is composed of a finite number of closed intervals, each corresponding to a finite number of branches. Since H_i are mechanical Hamiltonians, $\omega_i(\cdot) > 0$, $i = 1, 2$, and thus $H_i^{-1}(\cdot)$ are uniquely defined on each branch of the Liouville foliation [21, 8, 2]. For all level sets in $\mathbb{H}_2^{R,\delta}(H)$, by the S3B assumption (no parabolic points), there exists a $K > 0$ such that for all $I \in H_2^{-1}(\mathbb{H}_2^{R,\delta}(H))$ the frequencies $\omega_2(I) = H_2'(I)$ are bounded from below:

$$\omega_2 \geq \left| \frac{K}{\ln(\delta)} \right| \quad (7)$$

The notation $H_2^{-1}(\mathbb{H}_2^{R,\delta}(H))$ refers to the multi-valued set defined on all (finite number of) relevant branches, and H_2^{-1} is well defined even when $\delta \rightarrow 0$ (though it may be discontinuous at separatrices). It follows that the measure of the excluded set of action values I , similarly to the corresponding set of excluded energies in (4) goes to 0 as $\delta \rightarrow 0$ - see Theorem 2.6.

2.1 Integrable impact return map

When the wall is vertical ($b \neq 0, \epsilon_w = 0$), namely, it respects the separability symmetry of the underlying integrable Hamiltonian flow, one immediately concludes, by the rule of elastic reflection and the symmetry of the kinetic energy term, integrability:

Lemma 2.2. (*Integrability*) *When $\epsilon_r = \epsilon_w = 0$ the dynamics of the impact system are integrable.*

The vertical wall produces the additional singular level sets that correspond to tangent trajectories with H_1 energy $V_1(0)$. Generically, such level sets do not coincide with the singular level sets of H_1 , namely:

Definition 2.3. The vertical wall position is regular if $V_1'(q_1^w = 0) \neq 0$ and $V_1(q_1^w) \neq V_1(q_{1s,j})$, $j = 1, \dots, n_{1s}$.

Since H_1 is of the mechanical form, it follows that for any given H_1 there exists at most a single Liouville leaf in the (q_1, p_1) plane which intersects the wall at $q_1 = q_1^w = 0$, called hereafter

the *intersecting leaf*. In particular, for a family of intersecting leaves, the value of $|p_1^w(H_1)| = \sqrt{H_1 - V_1(0)}$ is uniquely defined and is monotone in H_1 for all $H_1 > H_{1tan} = V_1(0)$ as is the dependence on $J = H_1^{-1}(\cdot)$ on such intersecting leaves. For fixed energy $H = H_1 + H_2$, a branch can be either intersecting (meaning that all leaves of this branch intersect the wall), non-intersecting, or tangent. Namely, the location of the perpendicular wall determines uniquely *the tangent branch*; for regular wall position, for each energy value $H = h \geq V_1(0) + \min V_2$, there exists a unique leaf within the level set $H_1 = H_{1tan}, H_2 = h - H_{1tan}$, at which a tangency occurs. For a fixed energy H , we call the branch corresponding to this leaf *the tangent branch*, and on this branch $J \approx J_{tan} = H_1^{-1}(V_1(0))$ uniquely defines the leaves. In conclusion, we establish:

Lemma 2.4. *In the unperturbed vertical wall case ($\epsilon_r = \epsilon_w = 0$) with regular wall position, for the flow restricted to the tangent and intersecting branches, tangency occurs at $J_{tan} = H_1^{-1}(V_1(0))$ whereas impacts occur iff $J \geq J_{tan}$.*

Hereafter, unless specified otherwise, we consider the dynamics only on the tangent and intersecting branches (for the integrable dynamics all other branches are unaffected by the impact).

Next, a return map of the integrable impact system is constructed and it is proven that it is C^r smooth and satisfies the twist condition for most initial conditions. Since the motion occurs to the right of the vertical wall and the impact occurs whenever $q_1 = 0$, choosing the cross-section $\Sigma = \{(q_1, p_1) : p_1 = 0, \dot{p}_1 < 0\}$ ensures that in each iteration of the return map at most a single collision with the wall occurs. The return map to Σ , for the system without the impact is simply:

$$\begin{cases} I' &= I(T_1(J)) = I \\ \theta' &= \theta(T_1(J)) = \theta + \omega_2(I) \cdot T_1(J(H, I)) = \theta + \frac{T_1(J(H, I))}{T_2(I)} \cdot 2\pi \end{cases} \quad (8)$$

where $J = J(H, I) = H_1^{-1}(H - H_2(I))$, $T_1(J) = \frac{2\pi}{\omega_1(J)}$ and $T_2(I) = \frac{2\pi}{\omega_2(I)}$ are well defined for $I \in H_2^{-1}(\mathbb{H}_2^{R, \delta}(H))$ for small $\delta > 0$. Similarly, the corresponding return map $\mathcal{F}_0 : (I, \theta) \rightarrow (I', \theta')$ of the integrable impact system is defined for $I \in H_2^{-1}(\mathbb{H}_2^{R, \delta}(H))$ by:

$$\begin{cases} I' = I \\ \theta' = \theta + \omega_2(I) \cdot (T_1(J) - \Delta t_{travel}(J)) = \theta + 2\pi \frac{\tilde{T}_1(J)}{T_2(I)} \equiv \theta + \Theta(I, J(H, I)) \end{cases} \quad (9)$$

with

$$\Delta t_{travel}(J) = \begin{cases} 2 \int_{q_{1min}(J)}^0 \frac{dq_1}{\sqrt{2(H_1(J) - V_1(q_1))}} & \text{impact } (J > J_{tan}) \\ 0 & \text{no impact, tangency } (J \leq J_{tan}) \end{cases} \quad (10)$$

where $q_{1min}(J)$ is the minimal q_1 value on the chosen intersecting leaf that satisfies $V_1(q_{1min}) = H_1(J)$, i.e. the leftmost point of the trajectory (outside the billiard). Namely, Δt_{travel} is the time of travel outside the billiard which is lost due to the impact (see Figure 1) and $\tilde{T}_1(J) =$

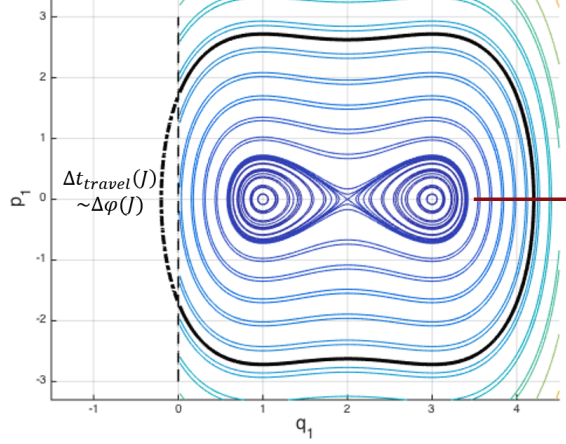


Figure 1: Isoenergetic curves in (q_1, p_1) , with an impacting trajectory emphasized in black. The wall is at $q_1^w = 0$ (dashed line), and the cross-section Σ corresponding to the relevant intersecting branch is drawn in red. The impact causes a jump in the angle $\Delta\varphi$, which is proportional to the time of travel Δt_{travel} outside the billiard, i.e. the travel time from p_1 to $-p_1$ at the impact point had there been no wall. The Hamiltonian H_1 in this figure corresponds to the undamped Duffing oscillator - see section 4.

$T_1(J) - \Delta t_{travel}(J)$ is the new period time in J . Generically, we expect that the level set of $H_2 = H - V_1(0)$ is regular:

Definition 2.5. H is δ -regular with respect to the wall position if $V_1(0) \in \mathbb{H}_1^{R,\delta}(H)$.

For regular wall position, for sufficiently small δ , there are at most a finite number of δ -intervals for which H is not regular, corresponding to the energy surfaces at which $H - V_1(0)$ are close to $V_2(q_{2s,j})$ for some j . For δ -regular H values, denote by $I_{tan}(H) = H_2^{-1}(H - V_1(0))$ and notice that impacting trajectories, corresponding to $J > J_{tan}$, yield $I < I_{tan}(H)$. We now establish:

Theorem 2.6. (Smoothness of (9)) Consider a Hamiltonian H of the form Eq. (1) with an S3B integrable structure H_{int} and a regular wall position (Def. 2.3), with $\epsilon_r = \epsilon_w = 0$. Fix $\delta > 0, \rho > 0$, and consider a δ -regular energy level $H < b$. Then for I in $H_2^{-1}(\mathbb{H}_2^{R,\delta}(H))$, excluding a ρ -interval centered at I_{tan} (so $I \in H_2^{-1}(\mathbb{H}_2^{R,\delta}(H)) \setminus \mathcal{N}_\rho(I_{tan}(H))$), the return map $\mathcal{F}_0 : (I, \theta) \rightarrow (I', \theta')$ is symplectic and C^r smooth, i.e. $\exists M_r(\rho, \delta) < \infty$ such that $\|\Theta(I, J(H, I))\|_{C^r} < M_r(\rho, \delta)$. Moreover, the regular set $H_2^{-1}(\mathbb{H}_2^{R,\delta}(H)) \setminus \mathcal{N}_\rho(I_{tan}(H))$ on which the return map (9) is C^r smooth is of $\mathcal{O}(1)$ in δ, ρ .

Proof. This is a result of the property of smooth dependence on initial conditions in ODEs and the assumed structure of the flow. For impact away from tangency, the cross-sections $\{q_1 = 0, p_1 < 0\}$, $\{q_1 = 0, p_1 > 0\}$ are transverse to the flow. The travel time $\Delta t_{travel}(J)$ corresponds to the travel time between the former and the latter transverse cross-sections. Since neighborhoods of separatrices are excluded, this travel time is finite and depends smoothly on initial conditions.

Finally, it follows from (5,7) that for small δ , the measure of the set of excluded action values satisfies:

$$|H_2^{-1}\left(\bigcup_{j=1}^{n_{2s}} \mathcal{N}_\delta(H_2(q_{2s,j}, 0)) \cup \bigcup_{j=1}^{n_{1s}} \mathcal{N}_\delta(H - H_1(q_{1s,j}, 0))\right) \cup \mathcal{N}_\rho(I_{tan}(H))| \leq \mathcal{O}(\delta |\ln(\delta)|, \rho) \quad (11)$$

as for each neighborhood of $q_{1s,j}, j = 1, \dots, n_{1s}$ an $\mathcal{O}(\delta)$ neighborhood of I values is excluded, whereas for each neighborhood of $q_{2s,j}, j = 1, \dots, n_{2s}$ the excluded I values consist of an $\mathcal{O}(\delta |\ln(\delta)|)$ neighborhood (Eq. 7). Hence, as $\delta, \rho \rightarrow 0$, for $H = \mathcal{O}(1)$ as considered here, the set of regular action values $I \in H_2^{-1}(\mathbb{H}_2^{R,\delta}(H)) \setminus \mathcal{N}_\rho(I_{tan}(H))$ is of $\mathcal{O}(1)$ as claimed. \square

Near tangency the map \mathcal{F}_0 is symplectic and C^0 - continuous but not smooth.

Remark. For impacting trajectories, the new period time in J , $\tilde{T}_1(J) = 2 \int_0^{q_{1max}(J)} \frac{dq_1}{\sqrt{2(H_1(J) - V_1(q_1))}}$ can also be calculated for level sets near a separatrix when the saddle point is outside the billiard (so the travel time on the trajectory inside the billiard is finite), or, similarly, for potentials with unbounded level sets where the billiard serves to effectively bound the energy level set (i.e. level sets are unbounded only on the outer side of the wall). The theorem can therefore be extended to such cases following suitable alterations to the initial assumptions.

The return map (9) satisfies the twist condition away from the non-twist set:

Definition 2.7. The Non-Twist set for a given energy level H is:

$$\mathbf{I}_{NT}(H) = \{I \in H_2^{-1}(\mathbb{H}_2^{R,\delta}(H)) \mid H_1(J(H, I)) + H_2(I) = H, \frac{d}{dI}\left(\frac{\tilde{T}_1(J)}{T_2(I)} \cdot 2\pi\right) = 0\} \quad (12)$$

Theorem 2.8. (*The Regular-Twist set*) Consider a Hamiltonian H of the form Eq. (1) with an S3B integrable structure H_{int} and a regular wall position, with $\epsilon_r = \epsilon_w = 0$. Fix $\delta > 0, \rho > 0$, and consider a δ -regular energy level $H < b$. Then, for sufficiently small δ, ρ , the regular-twist set $H_2^{-1}(\mathbb{H}_2^{R,\delta}(H)) \setminus \mathcal{N}_\rho(I_{tan}(H) \cup \mathbf{I}_{NT}(H))$ on which the return map (9) is a C^r twist map is of $\mathcal{O}(1)$ in δ, ρ .

Proof. Generically, the set $\mathbf{I}_{NT}(H)$ is a discrete, finite set, hence excluding its ρ -intervals leaves, for sufficiently small ρ , a set of I values of measure of $\mathcal{O}(1)$. \square

The set $\mathbf{I}_{NT}(H) \cap \{I > I_{tan}(H)\}$ corresponds to non-impacting tori which are non-twist due to the underlying system, whereas the set $\mathbf{I}_{NT}(H) \cap \{I < I_{tan}(H)\}$ corresponds to tori that lose their twist due to the impact.

Using the implicit relation $J = J(H, I)$, after some algebra, the twist condition becomes:

$$\frac{d\Theta}{dI} = 2\pi \cdot \frac{-T_1(J) \cdot \tilde{T}'_1(J) - \tilde{T}_1(J) \cdot T'_2(I)}{T_2^2(I)} \neq 0 \quad (13)$$

Since $T_1(J), \tilde{T}_1(J), T_2(I)$ are always non-negative, a necessary condition to have a non-twist torus is that $\tilde{T}'_1(J)$ and $T'_2(I)$ have opposite signs (see also section 4).

Proposition 2.9. *The non-twist set may only occur in regions where the modified periods in each d.o.f. have opposite monotonicity property: $I \in \mathbf{I}_{NT}(H) \Rightarrow \tilde{T}'_1(J) \cdot T'_2(I) \leq 0$ (where $J = J(H, I)$).*

Finally, notice that the rotation number for the twist map (9) changes at $I = I_{tan}(H)$ from its impacting value $\frac{\tilde{T}_1(J)}{T_2(I)}$ to its non-impacting value $\frac{T_1(J)}{T_2(I)}$, namely the resonance surfaces change non-smoothly at $I = I_{tan}$.

3 Near integrability results

In the smooth case without the impact, when $\epsilon_r \neq 0$ is small, the usual near-integrable dynamics emerge, including the existence of KAM tori, resonances near the rational values of $\frac{T_1(J)}{T_2(I)}$ and various types of homoclinic chaos near the singular level sets [2, 24, 23, 15].

Utilizing the construction of the return map (9) which is an integrable, C^r smooth, symplectic twist map for the vertical wall case, we now show that under small perturbations $\epsilon = (\epsilon_r, \epsilon_w) \neq 0$, the perturbed return map, \mathcal{F}_ϵ , away from the singularities, is a C^r -symplectic map (the near singularities behavior will be studied elsewhere). Furthermore, we also establish that this map is C^r -close to the integrable one, hence KAM theory applies and invariant near-integrable regions in phase space can be identified. More precisely:

Theorem 3.1. *Consider a Hamiltonian H of the form Eq. (1) with an S3B integrable structure H_{int} and a regular wall position. Fix $\delta > 0, \rho > 0$, let $\epsilon = (\epsilon_r, \epsilon_w)$ and $\varepsilon = \|\epsilon\|$, and consider a δ -regular energy level $H < b$. Then for $I \in H_2^{-1}(\mathbb{H}_2^{R,\delta}(H)) \setminus \mathcal{N}_\rho(I_{tan})$, for all θ , for sufficiently small ε the return map $\mathcal{F}_\epsilon : (I, \theta) \rightarrow (I', \theta')$ is symplectic, C^r smooth and $\varepsilon - C^r$ close to the unperturbed impact return map \mathcal{F}_0 of Eq. (9). Namely, for all (I, θ) in this bounded domain, there exists $\varepsilon_0(H, \delta, \rho) > 0$, such that for all $\varepsilon \in [0, \varepsilon_0(H, \delta, \rho))$:*

$$\mathcal{F}_\epsilon : \begin{cases} I' = I + \varepsilon f(I, \theta; \epsilon) \\ \theta' = \theta + \Theta(I, J(H, I)) + \varepsilon g(I, \theta; \epsilon) \end{cases} \quad (14)$$

with f, g 2π -periodic in θ , $f, g \in C^r$.

Proof. We first show that the perturbed return map $\mathcal{F}_\epsilon : (I, \theta) \rightarrow (I', \theta')$ can be decomposed to three maps:

$$\mathcal{F}_\epsilon = \Phi_{\epsilon_r}^{[t_\epsilon^*, t_\epsilon^{**}]} \circ S_{\epsilon_w} \circ \Phi_{\epsilon_r}^{[0, t_\epsilon^*]} \quad (15)$$

where Φ denotes the smooth Hamiltonian flow corresponding to system without the impact $H(\cdot; \epsilon_r, b = 0)$ which governs the dynamics before and after impact, t_ϵ^* and t_ϵ^{**} denote the time of impact with

the wall and the time of return to the cross-section respectively and S is the impact (gluing) map. The subscript indicates the dependence on the two different types of perturbations.

Since $\Phi_{\epsilon_r}^{[0,t]}$ is the C^r smooth Hamiltonian flow corresponding to the Hamiltonian $H(\cdot; \epsilon_r, b = 0)$ which is C^r close to the unperturbed smooth Hamiltonian flow $H(\cdot; \epsilon_r = 0, b = 0)$ for any finite t , by considering I values only in the regular domain of the unperturbed flow, we insure that for sufficiently small ϵ_r the two smooth flows are $\epsilon_r - C^r$ close on the finite time interval $[0, t_0^* + 1]$, where t_0^* denotes the finite unperturbed impact time. Since, away from $t = \{0, t_0^*\}$, the unperturbed segment of the flow for the considered regular I values is bounded away from Σ and from the section $q_1 = 0$, for sufficiently small ϵ_r the same statement holds for the perturbed smooth flow. Hence, for sufficiently small ϵ_w there is no crossing of Σ or the wall coordinate occurring at t -values in the interior of the interval $(0, t_0^*)$. It follows that for sufficiently small ε , the perturbed first impact with the perturbed wall occurs before the trajectory returns to Σ , is transverse, and the perturbed travel time t_ϵ^* is finite and $\varepsilon - C^r$ close to t_0^* . Hence, for sufficiently small ϵ_w , the gluing map S_{ϵ_w} is C^r smooth (for a C^{r+1} smooth boundary [9]) regardless of the form of the deformation or tilt of the wall, and, for sufficiently small ε , the composition $S_{\epsilon_w} \circ \Phi_{\epsilon_r}^{[0,t_\epsilon^*]}$ is $\varepsilon - C^r$ close to the unperturbed composition, $S_0 \circ \Phi_0^{[0,t_0^*]}$. Namely, the perturbed trajectory just after the impact is $\varepsilon - C^r$ close to the unperturbed trajectory after impact.

It follows that the perturbed trajectory which is propagated by the perturbed flow Φ_{ϵ_r} remains $\varepsilon - C^r$ close to the unperturbed impact trajectory for finite times (e.g. past the unperturbed return time to the transverse cross section Σ), and hence, by similar considerations as above, cannot collide with the wall or cross Σ at t values which are bounded away from t_0^* and t_0^{**} respectively. In particular, we obtain that the perturbed return time t_ϵ^{**} is finite and $\varepsilon - C^r$ close to t_0^{**} .

Summarizing, for $I \in H_2^{-1}(\mathbb{H}_2^{R,\delta}(H)) \setminus \mathcal{N}_\rho(I_{tan})$, for all θ , the return map \mathcal{F}_ϵ to Σ includes a single transverse collision with the perturbed wall at $t_\epsilon^* = t_0^* + \mathcal{O}(\varepsilon)$ and thus the return map is of the form $\mathcal{F}_\epsilon = \Phi_{\epsilon_r}^{[t_\epsilon^*, t_\epsilon^{**}]} \circ S_{\epsilon_w} \circ \Phi_{\epsilon_r}^{[0, t_\epsilon^*]}$ and is $\varepsilon - C^r$ close to the unperturbed impact return map $\mathcal{F}_0 = \Phi_0^{[t_0^*, t_0^{**}]} \circ S_0 \circ \Phi_0^{[0, t_0^*]}$ given by Eq. (9). \square

Note that the return times and closeness results statements are non-uniform in H . Establishing asymptotic results for large H requires more careful analysis of the bounds and constants appearing in the proof and will be deferred to later studies.

Corollary 3.2. *For fixed H and $\delta, \rho > 0$, consider a circle which is bounded away from separatrices, tangencies and the non-twist set, i.e. I_0 belongs to the closed "good" set $I_0 \in H_2^{-1}(\mathbb{H}_2^{R,\delta}(H)) \setminus (\mathcal{N}_\rho(I_{tan}) \cup \mathcal{N}_\rho(\mathbf{I}_{NT}(H))) \equiv S_g(H, \delta, \rho)$. Furthermore, assume $\Theta(I_0, J(H, I_0))/2\pi$ is (c, ν) -Diophantine*

$$\left| \Theta(I_0, J(H, I_0)) - \frac{2\pi m}{n} \right| > cn^{-\nu-1} \quad \forall m, n \in \mathbb{Z} \quad (16)$$

where $1 < \nu < \frac{1}{2}(r - 1)$. Then, there exists $\varepsilon_1(H, \delta, \rho; c, \nu)$ such that for all $\varepsilon < \varepsilon_1$ there exists

a perturbed invariant circle $(I_\varepsilon(\theta), \theta)$ with rotation number $\frac{\tilde{T}_1(J(H, I_0))}{T_2(I_0)}$ which is ε/c close to the unperturbed circle $I = I_0$. Furthermore, the same result is valid for small c as long as c is at least of $\mathcal{O}(\sqrt{\varepsilon})$.

Proof. From Theorem 3.1, the map (14) on $S_g(H, \delta, \rho)$ is a C^r perturbation of an integrable twist map. It remains to show that the perturbed dynamics remain bounded away from tangency and separatrices - if this is shown, then the above corollary follows directly from KAM type results (see [2, 24, 10]) applied to the map (14). Indeed, notice that $S_g(H, \delta, \rho) \subset S_g(H, \delta/2, \rho/2)$ so the upper bounds on ε of Theorem 3.1 for these sets satisfy $\varepsilon_0(H, \delta, \rho) > \varepsilon_0(H, \delta/2, \rho/2)$. Taking $\varepsilon < \varepsilon_0(H, \delta/2, \rho/2)$, insures that if $I_0 \in S_g(H, \delta, \rho)$ then it is at least Δ away from the boundary of $S_g(H, \delta/2, \rho/2)$, where $\Delta = \min(\rho/4, K_1\delta, K_2\delta|\ln(2\delta)|)$ and $K_{1,2}(H)$ are some constants depending on the unperturbed rotation rates (see Eq. 7, 11). It follows that the map (14) is smooth in at least an $\mathcal{O}(\Delta)$ neighborhood for all $I_0 \in S_g(H, \delta, \rho)$. Hence, by KAM theory, there exists $\varepsilon^*(H, \delta, \rho; c, \nu) < \varepsilon_0(H, \delta/2, \rho/2)$, such that for all $\varepsilon < \varepsilon^*$ near every $I_0 \in S_g(H, \delta, \rho)$ with c, ν -Diophantine $\Theta(I_0, J(H, I_0))/2\pi$, there exists a perturbed invariant curve with $I_\varepsilon(\theta) = I_0 + \mathcal{O}(\frac{\varepsilon}{c})$ with the same rotation number as I_0 . Since c is at least of $\mathcal{O}(\sqrt{\varepsilon})$, there exists $K > 0$ such that $\frac{\varepsilon}{c} < K\sqrt{\varepsilon}$. Taking $\varepsilon < \varepsilon_1(H, \delta, \rho; c, \nu) = \min(\varepsilon^*(H, \delta, \rho; c, \nu), (\frac{\Delta}{K})^2)$ insures that $K\sqrt{\varepsilon} < \Delta$, so the perturbed circle remains within the regular region $S_g(H, \delta/2, \rho/2)$ in which the map (14) is smooth, as required. \square

Corollary 3.3. *For sufficiently small ε , the complement to the set of all tori I_0 belonging to an energy surface H and satisfying the conditions of Corollary 3.2, namely the set of tori which do not necessarily persist under ε perturbations is of $\mathcal{O}(\sqrt{\varepsilon}, \rho, \delta \ln \delta)$.*

Proof. The complement to the set $S_g(H, \delta, \rho)$, namely the δ -neighborhoods of separatrices and ρ -neighborhoods of tangency and non-twist tori, are of $\mathcal{O}(\rho, \delta \ln \delta)$, see proof of Theorem 2.6. For $I_0 \in S_g(H, \delta, \rho)$, by Corollary 3.2, KAM theorem [2] may be applied, hence in $S_g(H, \delta, \rho)$ the complement set is the resonant set, and its measure is of $\mathcal{O}(\sqrt{\varepsilon})$. \square

The destroyed, resonant tori correspond to rational values of the modified rotation number $\frac{\tilde{T}_1(J)}{T_2(I)}$. Notice that the impact causes a shift in the resonant frequencies.

The excluded sets (neighborhoods of separatrices, of the tangent torus and of the non-twist tori) correspond to a finite, discrete number of singular $I(H)$ values. As $\varepsilon \rightarrow 0$, the size of these sets, which is controlled by δ, ρ , can be taken to tend slowly to 0 as well. The proof of corollary 3.2 which utilizes KAM theory implies that in such a case δ, ρ must be at least of $\mathcal{O}(\sqrt{\varepsilon})$. Finding the optimal power in ε is left for future studies. As the system is a 2 d.o.f system, this implies that the phase space can be divided into invariant regions of motion [2].

There are two cases in which the form of the perturbed map for I may be found. The first of which is the case of a perpendicular wall with an additional regular perturbation - $\epsilon_w = 0$,

so $\varepsilon = \varepsilon_r$. We introduce the following notation: let $z(t) = (q_1(t), p_1(t), q_2(t), p_2(t))$ and denote the impacting trajectory in the perturbed system by $z_\varepsilon(t) = \Phi_{\varepsilon_r}^{[0,t]} z(0)$, for $0 \leq t < t_\varepsilon^*$, and $z_\varepsilon^{im}(t) = \Phi_{\varepsilon_r}^{[t_\varepsilon^*,t]} \circ S \circ \Phi_{\varepsilon_r}^{[0,t_\varepsilon^*]} z(0)$ for $t_\varepsilon^* \leq t \leq t_\varepsilon^{**}$. Denote similarly by $z_0^{im}(t)$ the trajectory in the unperturbed impact system. Finally, denote by $z_0^{sm}(t) = \Phi_0^{[0,t]} z(0)$ the smooth, unperturbed, non-impacting trajectory. From Theorem 3.1 above, we have:

Corollary 3.4. *Consider the settings of theorem 3.1, with $\varepsilon_w = 0$ and ε_r sufficiently small. Let $\bar{t}_{min} = \min(t_0^*, t_{\varepsilon_r}^*)$, $\bar{t}_{max} = \max(t_0^*, t_{\varepsilon_r}^*)$. Then:*

$$z_{\varepsilon_r}(t) = \begin{cases} z_0^{im}(t) + \varepsilon_r z_1^{im}(t) + \mathcal{O}(\varepsilon_r^2) & t \in [0, \bar{t}_{min}] \cup [\bar{t}_{max}, t_{\varepsilon_r}^{**}] \\ \begin{cases} z_0^{sm}(t) + \varepsilon_r z_1^{sm}(t) + \mathcal{O}(\varepsilon_r^2) & \bar{t}_{min} = t_0^* \\ (q_{1,0}^{sm}(t + \Delta t_{travel}), p_{1,0}^{sm}(t + \Delta t_{travel}), q_{2,0}^{sm}(t), p_{2,0}^{sm}(t)) + \mathcal{O}(\varepsilon_r) & \bar{t}_{max} = t_0^* \end{cases} & t \in [\bar{t}_{min}, \bar{t}_{max}] \end{cases} \quad (17)$$

Where Δt_{travel} is as in Theorem 2.6, calculated for the unperturbed impacting trajectory, and z_1 solves the first variational equation along the corresponding trajectory.

In other words, for $\varepsilon = \varepsilon_r$, the perturbed trajectory $z_{\varepsilon_r}(t)$ and the unperturbed trajectory $z_0^{im}(t)$ are $\mathcal{O}(\varepsilon_r)$ close except for an $\mathcal{O}(\varepsilon_r)$ time interval where one trajectory has already undergone impact and the other has not, in which case the perturbed trajectory can be approximated by the respective continuation of the unperturbed trajectory outside the billiard.

Theorem 3.5. *Consider a Hamiltonian H of the form Eq. (1) with an S3B integrable structure H_{int} and a regular wall position, with $\varepsilon_w = 0$. Fix $\delta > 0$, $\rho > 0$, and consider a δ -regular energy level H . Then for $I \in H_2^{-1}(\mathbb{H}_2^{R,\delta}(H)) \setminus \mathcal{N}_\rho(I_{tan})$, for all θ , for sufficiently small ε_r , the function f of the change in I in the return map (14) has the following form:*

$$f(I, \theta; \varepsilon_r) = \frac{1}{\omega_2(I)} \int_0^{\tilde{T}_1(J(I,H))} \left(\frac{\partial V_r}{\partial q_2} p_2 \right)_{z_0^{im}(t)} dt + \mathcal{O}(\varepsilon_r) \quad (18)$$

Proof. Consider the evolution in time of I under the perturbed system before, during and after impact (see Figure 2). Before and after impact the motion is described by the smooth, near integrable Hamiltonian $H(\cdot; \varepsilon_r, b = 0)$ (Theorem 3.1 and Corollary 3.4) and at impact, as the wall is perpendicular, I is unchanged. With no loss of generality, we consider the case $\bar{t}_{min} = t_0^* < t_{\varepsilon_r}^*$ (the other case may be similarly treated). The evolution of I before the perturbed impact time $t_{\varepsilon_r}^*$

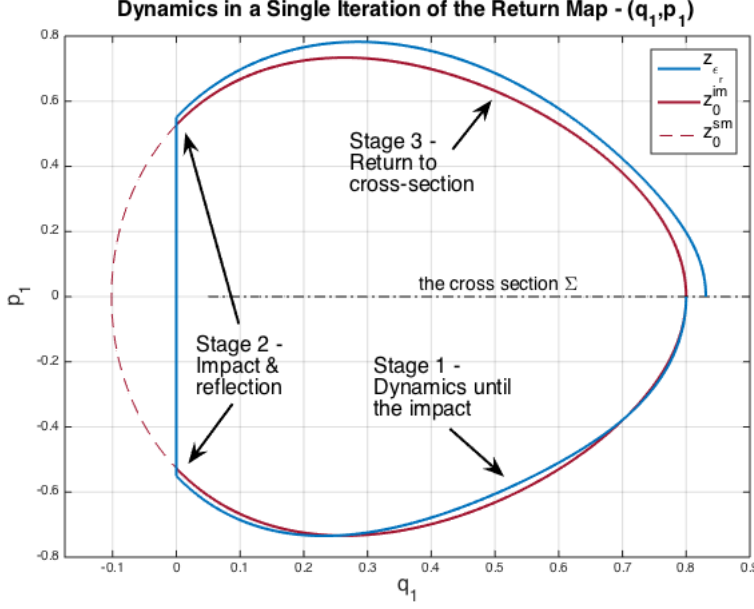


Figure 2: The perturbed impacting trajectory z_{ϵ_r} (blue), unperturbed impacting trajectory z_0^{im} (crimson) and unperturbed smooth trajectory z_0^{sm} (dashed crimson) during a single iteration of the return map to the cross-section Σ , projected to the (q_1, p_1) phase space, for the case of a perpendicular wall and a small regular perturbation. The wall is at $q_1 = 0$.

may be approximated by the evolution along the unperturbed trajectory until time t_0^* :

$$\begin{aligned}
 I^* &= I(t_{\epsilon_r}^*) = I + \int_0^{t_{\epsilon_r}^*} \{I, H_{int} + \epsilon_r V_r\} |_{z_{\epsilon_r}(t)} dt = I + \int_0^{t_0^*} + \int_{t_0^*}^{t_{\epsilon_r}^*} \{I, \epsilon_r V_r\} |_{z_{\epsilon_r}(t)} dt \\
 &= I + \epsilon_r \int_0^{t_0^*} \{I, V_r\} |_{z_0^{im}(t)} dt + \mathcal{O}(\epsilon_r^2)
 \end{aligned} \tag{19}$$

where we used $\{I, H_{int}\} = 0$, Theorem 3.1 and Corollary 3.4. I^* does not change at impact, and the evolution back to the cross-section Σ after the impact may be calculated similarly:

$$\begin{aligned}
 I' &= I(t_{\epsilon_r}^{**}) = I(t_{\epsilon_r}^*) + \int_{t_{\epsilon_r}^*}^{t_{\epsilon_r}^{**}} \{I, H_{int} + \epsilon_r V_r\} |_{z_{\epsilon_r}(t)} dt \\
 &= I^* + \int_{t_{\epsilon_r}^*}^{t_0^{**}} \{I, \epsilon_r V_r\} |_{z_{\epsilon_r}(t)} dt + \int_{t_0^{**}}^{t_{\epsilon_r}^{**}} \{I, \epsilon_r V_r\} |_{z_{\epsilon_r}(t)} dt \\
 &= I^* + \epsilon_r \int_{t_{\epsilon_r}^*}^{t_0^{**}} \{I, V_r\} |_{z_0^{im}(t)} dt + \mathcal{O}(\epsilon_r^2) = I^* + \epsilon_r \int_{t_0^*}^{t_0^{**}} \{I, V_r\} |_{z_0^{im}(t)} dt + \mathcal{O}(\epsilon_r^2).
 \end{aligned} \tag{20}$$

Finally, substituting $\{I, V_r\} = \frac{\partial V_r}{\partial \theta}$ and since $t_0^{**} = \tilde{T}_1(J)$ (see (9)):

$$\begin{aligned} I' &= I + \epsilon_r \int_0^{t_0^{**}} \frac{\partial V_r}{\partial \theta} \Big|_{z_0^{im}(t)} dt + \mathcal{O}(\epsilon_r^2) = I + \epsilon_r \int_0^{t_0^{**}} \frac{\partial V_r}{\partial q_2} \cdot \frac{\partial q_2}{\partial \theta} \Big|_{z_0^{im}(t)} dt + \mathcal{O}(\epsilon_r^2) \\ &= I + \epsilon_r \int_0^{\tilde{T}_1(J)} \frac{\partial V_r}{\partial q_2} \cdot \frac{\dot{q}_2}{\dot{\theta}} \Big|_{z_0^{im}(t)} dt + \mathcal{O}(\epsilon_r^2) = I + \epsilon_r \frac{1}{\omega_2(I)} \int_0^{\tilde{T}_1(J)} \left(\frac{\partial V_r}{\partial q_2} p_2 \right) \Big|_{z_0^{im}(t)} dt + \mathcal{O}(\epsilon_r^2) \end{aligned} \quad (21)$$

□

The other case in which explicit form of the leading order term in I can be written, is the case of a tilted, near perpendicular straight wall and a small regular perturbation ($q_1^w = \epsilon_w Q^w(q_2^w) = \epsilon_w q_2^w$, ϵ_w, ϵ_r small). In fact, we show next that by rotating the coordinate system this case reduces to an example of the previous one. Consider first a tilted wall with no additional perturbation to the potential, so $\epsilon_r = 0$ and $q_1^w = \epsilon_w q_2^w$, ϵ_w small. The symplectic change of coordinates, of rotating the axes by $\alpha = \arctan(\epsilon_w)$:

$$\tilde{q} = Rq, \quad \tilde{p} = Rp, \quad R = \begin{pmatrix} \cos \alpha & -\sin \alpha \\ \sin \alpha & \cos \alpha \end{pmatrix} \quad (22)$$

makes the wall perpendicular to the new \tilde{q}_1 axis, i.e. $\tilde{Q}^w = Q^w(\tilde{q}_2^w) = 0$. Substituting the new coordinates in the Hamiltonian, we obtain:

$$\begin{aligned} \tilde{H}(\tilde{q}_1, \tilde{q}_2, \tilde{p}_1, \tilde{p}_2) &= H(\cos \alpha \cdot \tilde{q}_1 + \sin \alpha \cdot \tilde{q}_2, -\sin \alpha \cdot \tilde{q}_1 + \cos \alpha \cdot \tilde{q}_2, \cos \alpha \cdot \tilde{p}_1 + \sin \alpha \cdot \tilde{p}_2, -\sin \alpha \cdot \tilde{p}_1 + \cos \alpha \cdot \tilde{p}_2) \\ &= \frac{\tilde{p}_1^2}{2} + \frac{\tilde{p}_2^2}{2} + V_1(\cos \alpha \cdot \tilde{q}_1 + \sin \alpha \cdot \tilde{q}_2) + V_2(-\sin \alpha \cdot \tilde{q}_1 + \cos \alpha \cdot \tilde{q}_2) + b \cdot V_b(\tilde{q}_1, \tilde{q}_2) \end{aligned} \quad (23)$$

$V_{1,2}$ are C^{r+1} functions and therefore can be expanded around \tilde{q}_1, \tilde{q}_2 respectively:

$$\begin{aligned} V_1(q_1) &= V_1(\cos \alpha \cdot \tilde{q}_1 + \sin \alpha \cdot \tilde{q}_2) = V_1(\tilde{q}_1) + (\tilde{q}_1 - (\cos \alpha \cdot \tilde{q}_1 + \sin \alpha \cdot \tilde{q}_2)) \cdot V_1'(\tilde{q}_1) \\ &\quad + (\tilde{q}_1 - (\cos \alpha \cdot \tilde{q}_1 + \sin \alpha \cdot \tilde{q}_2)) \cdot h_1(\cos \alpha \cdot \tilde{q}_1 + \sin \alpha \cdot \tilde{q}_2) \\ V_2(q_2) &= V_2(-\sin \alpha \cdot \tilde{q}_1 + \cos \alpha \cdot \tilde{q}_2) = V_2(\tilde{q}_2) + (\tilde{q}_2 - (-\sin \alpha \cdot \tilde{q}_1 + \cos \alpha \cdot \tilde{q}_2)) \cdot V_2'(\tilde{q}_2) \\ &\quad + (\tilde{q}_2 - (-\sin \alpha \cdot \tilde{q}_1 + \cos \alpha \cdot \tilde{q}_2)) \cdot h_2(-\sin \alpha \cdot \tilde{q}_1 + \cos \alpha \cdot \tilde{q}_2) \end{aligned} \quad (24)$$

Where $h_1, h_2 \rightarrow 0$ as $\epsilon_w \rightarrow 0$. For ϵ_w small, the trigonometric functions can also be expanded:

$$\begin{aligned} V_1(\cos \alpha \cdot \tilde{q}_1 + \sin \alpha \cdot \tilde{q}_2) &= V_1(\tilde{q}_1) + \epsilon_w V_{1,rem}(\tilde{q}_1, \tilde{q}_2; \epsilon_w) \\ V_2(-\sin \alpha \cdot \tilde{q}_1 + \cos \alpha \cdot \tilde{q}_2) &= V_2(\tilde{q}_2) + \epsilon_w V_{2,rem}(\tilde{q}_1, \tilde{q}_2; \epsilon_w) \\ V_{rem}(\tilde{q}_1, \tilde{q}_2; \epsilon_w) &= V_{1,rem}(\tilde{q}_1, \tilde{q}_2; \epsilon_w) + V_{2,rem}(\tilde{q}_1, \tilde{q}_2; \epsilon_w) \end{aligned} \quad (25)$$

where $V_{rem}(\cdot)$ is C^r and in particular bounded on the perturbed energy surface (though non-uniformly in H). The form of the Hamiltonian in the new rotated coordinates is

$$\tilde{H}(\tilde{q}_1, \tilde{q}_2, \tilde{p}_1, \tilde{p}_2) = \frac{\tilde{p}_1^2}{2} + \frac{\tilde{p}_2^2}{2} + V_1(\tilde{q}_1) + V_2(\tilde{q}_2) + \epsilon_w V_{rem}(\tilde{q}_1, \tilde{q}_2; \epsilon_w) + b \cdot V_b(\tilde{q}_1; 0) \quad (26)$$

where, using the expansion in (24), we have:

$$V_{rem} = -\tilde{q}_2 \cdot V_1'(\tilde{q}_1) + \tilde{q}_1 \cdot V_2'(\tilde{q}_2) + \mathcal{O}(\epsilon_w) \quad (27)$$

namely, the integrable part of \tilde{H} , in the rotated coordinates, is exactly H_{int} . Notice that due to the expansion, the smoothness of the leading order perturbation term is reduced by one. We establish:

Corollary 3.6. *For H, ϵ_w and initial conditions $(\tilde{I}, \tilde{\theta})$ which satisfy the assumptions of Theorem 3.1 with $r > 4$, an impact by a near perpendicular straight wall is equivalent to the system with impact with a perpendicular wall and a small, regular perturbation. Moreover, the form of the change in \tilde{I} due to the wall tilt becomes (see Theorem 3.5):*

$$f(\tilde{I}, \tilde{\theta}; \epsilon_w) = \frac{1}{\omega_2(\tilde{I})} \int_0^{\tilde{T}_1(\tilde{J})} \left([-V_1'(\tilde{q}_1) + \tilde{q}_1 \cdot V_2''(\tilde{q}_2)] \tilde{p}_2 \right)_{\tilde{z}_0^{im}(t)} dt + \mathcal{O}(\epsilon_w) \quad (28)$$

Similarly, when both $\epsilon_w, \epsilon_r \neq 0$ and are of the same order, one finds that the Hamiltonian in the rotated coordinates corresponds to a system with a perpendicular wall and a small regular perturbation, comprised of a rotation term $\epsilon_w V_{rem}(\tilde{q}_1, \tilde{q}_2)$ and the original regular perturbation $\epsilon_r \tilde{V}_r(\tilde{q}_1, \tilde{q}_2; \epsilon_r, \epsilon_w)$. Using a similar expansion to (24), we have:

$$V_r(q_1, q_2; \epsilon_r) = V_r(\tilde{q}_1, \tilde{q}_2; \epsilon_r) + \epsilon_w \left(-\tilde{q}_2 \frac{\partial V_r}{\partial q_1}(\tilde{q}_1, \tilde{q}_2) + \tilde{q}_1 \frac{\partial V_r}{\partial q_2}(\tilde{q}_1, \tilde{q}_2) \right) + \mathcal{O}(\epsilon_w^2) := \tilde{V}_r(\tilde{q}_1, \tilde{q}_2; \epsilon_r, \epsilon_w) \quad (29)$$

Assuming that $\epsilon_r = c_r \epsilon$, $\epsilon_w = c_w \epsilon$, the form of the change in \tilde{I} becomes (see Theorem 3.5, equations (24,29)):

$$f(\tilde{I}, \tilde{\theta}; \epsilon) = \frac{1}{\omega_2(\tilde{I})} \int_0^{\tilde{T}_1(\tilde{J})} \left(\left[c_w [-V_1'(\tilde{q}_1) + \tilde{q}_1 \cdot V_2''(\tilde{q}_2)] + c_r \frac{\partial V_r}{\partial \tilde{q}_2} \right] \tilde{p}_2 \right)_{\tilde{z}_0^{im}(t)} dt + \mathcal{O}(\epsilon). \quad (30)$$

Soft impacts

For physical setups in which bodies at close range experience strong repulsion forces (e.g. the repelling forces between two colliding atoms) [27, 30, 20, 17], a better model for the strong repulsion than the singular hard-wall billiard potential is a smooth step potential. Hence, consider Hamiltonian systems similar to those discussed above, where the hard billiard is replaced by a

smooth potential whose softness is controlled by a small parameter ϵ_b :

$$H = H(\cdot; \epsilon_r, \epsilon_w, \epsilon_b, q^w, b) = H_{int}(q_1, p_1, q_2, p_2) + \epsilon_r V_r(q_1, q_2) + b \cdot V_b(q; \epsilon_w, \epsilon_b) \quad (31)$$

As $\epsilon_b \rightarrow 0$, the smooth (C^{r+1}) billiard potential $V_b(\cdot, \epsilon_b)$ becomes steeper at the wall (as $q - q^w \rightarrow 0^+$) and approaches the singular hard wall limit. For example, one can choose (see [27, 17] for additional examples):

$$V_{b,poly}(q; \epsilon_w, \epsilon_b) = \frac{\epsilon_b}{q_1 - \epsilon_w Q^w(q_2; \epsilon_w)} \quad (32)$$

$$V_{b,exp}(q; \epsilon_w, \epsilon_b) = \exp\left(-\frac{q_1 - \epsilon_w Q^w(q_2; \epsilon_w)}{\epsilon_b}\right) \quad (33)$$

Notice that in particular, on the wall, $\lim_{q \rightarrow q^w} b \cdot V_b(q; \epsilon_w, \epsilon_b) \geq b$ (this limit, which corresponds to the "barrier height", is infinite for the potential $V_{b,poly}$ and finite for $V_{b,exp}$). It has been shown [27, 17] that under some natural conditions on V_b , for trajectory segments that are bounded away from tangencies and have energies which are not too large (so they cannot cross the boundary), the smooth, soft impact flow and the piecewise-smooth, hard impact flow are C^r close on a section bounded away from the impact boundary. The detailed conditions of [17] and their realization in the context of the current setup are included, for completeness, in appendix B. Then, the results in [17] can be used to prove a somewhat weaker version of Theorem 3.1 that applies to the soft impact case (in particular, unless ϵ_b is taken to be very small, the form of the perturbed return map also depends on the errors gathered by the singular perturbation term, see corollary 3.8):

Theorem 3.7. *Consider a Hamiltonian H of the form Eq. (31) with an S3B integrable structure H_{int} , a regular wall position, and a soft billiard potential V_b satisfying conditions I-IV (see appendix B). Fix $\delta > 0, \rho > 0$, let $\epsilon = (\epsilon_r, \epsilon_w, \epsilon_b)$ and $\varepsilon = \|\epsilon\|$, and consider a δ -regular energy level H satisfying $H < H_{max}(b)$ (see appendix). Then for $I \in H_2^{-1}(\mathbb{H}_2^{R,\delta}(H)) \setminus \mathcal{N}_\rho(I_{tan})$, for all θ , for sufficiently small ε the return map $\mathcal{F}_\epsilon : (I, \theta) \rightarrow (I', \theta')$ is symplectic, C^r smooth and C^k close to the unperturbed impact return map \mathcal{F}_0 of Eq. (9) for any $k \leq r$. Namely, for all (I, θ) in this bounded domain, there exists $\varepsilon_b(H, \delta, \rho) > 0$ such that for all $\varepsilon \in [0, \varepsilon_b(H, \delta, \rho))$, $\mathcal{F}_\epsilon = \mathcal{F}_0 + o_{C^k}(1)$.*

Proof. Symplecticity and smoothness of the soft impact flow, and hence the map, are immediate. Since the transverse section Σ is bounded away from the wall, and since we consider orbits which are bounded away from being tangent, the C^k closeness of $\mathcal{F}_{(\epsilon_r, \epsilon_w, \epsilon_b)}$ and $\mathcal{F}_{(\epsilon_r, \epsilon_w, \epsilon_b=0^+)}$ follows from Theorem 1 in [17] (see appendix, where the conditions of Theorem 1 in [17] are shown to be satisfied here, and the bounds on H are shown to guarantee that for sufficiently small ε particles cannot cross the wall). The C^r closeness of $\mathcal{F}_{(\epsilon_r, \epsilon_w, \epsilon_b=0^+)}$ to \mathcal{F}_0 for sufficiently small ϵ_r, ϵ_w follows from Theorem 3.1. \square

Remark. Notice that the approximation of the near integrable map by the integrable one is weaker

here, as the error is $o(1)$ in ϵ_b , versus the $\mathcal{O}(\epsilon)$ error in Theorem 3.1. This is due to the singular nature of the soft billiard perturbation, as opposed to the regular perturbations of the Hamiltonian structure or the vertical wall shape. Error estimates for the hard billiard case have been calculated in [27] for some specific forms of V_b . These estimates may be extended to the soft impact case and used to derive an explicit formula for the first order approximation term to the soft impact return map. The exact formulation is left for future works. However, the existence of such estimates implies that there exists ϵ_b sufficiently small such that the error remains $\mathcal{O}(\epsilon)$, i.e.

Corollary 3.8. *There exists $\epsilon_{b,k}(\epsilon_r, \epsilon_w)$ such that for all $\epsilon_b < \epsilon_{b,k}$, under the conditions of Theorem 3.7, the soft impact return map \mathcal{F}_ϵ is $\epsilon - C^k$ close to \mathcal{F}_0 and in the special calculable cases the first order term in ϵ of the soft impact return map takes the corresponding forms (18), (28) or (30).*

For example, we conjecture that if for a given soft potential form the error estimate for C^k closeness as in [27] is of $\mathcal{O}(\epsilon^{k+2}/\sqrt{\epsilon_b})$, then for $\epsilon_b \leq \mathcal{O}(\epsilon_r^{k+2}, \epsilon_w^{k+2})$ the overall error would be of $\mathcal{O}(\epsilon)$ as required.

4 Example

Consider the Hamiltonian $H_{int} = \frac{p_1^2}{2} + \frac{p_2^2}{2} - \frac{\lambda^2}{2} \cdot (q_1 - q_{1s})^2 + \frac{1}{4} \cdot (q_1 - q_{1s})^4 + \frac{\omega^2}{2} \cdot (q_2 - q_{2s})^2$. In the (q_1, p_1) plane the Hamiltonian flow has a saddle point $(q_{1s}, 0)$ and a separatrix loop which encircles two symmetric centers - the undamped Duffing oscillator [24]; In (q_2, p_2) there is a single linear center (see Figure 3). The period in the (q_1, p_1) plane is piecewise monotone; it becomes infinite at the separatrix ($H_1 = 0$), where it reverses its direction of monotonicity: $T_1'(H_1) \cdot \text{sign}(H_1) < 0$ (see Figure 5). The period around the linear center is fixed: $T_2(H_2) = \frac{2\pi}{\omega}$. In the regular regions away from the separatrix, action-angle variables can be defined and $H_{int} = H_1(J) + \omega I$. The periods' relation $2\pi \frac{T_1(H_1)}{T_2(H_2)} = \omega T_1(H - \omega I)$ in these regions is monotone, and so the smooth return map (8) for H_{int} is a twist map. Consider now the impact system (1) with H_{int} as above and $\epsilon_r = \epsilon_w = 0$. The parameters q_{1s}, λ can be chosen such that the wall location is either inside or outside the separatrix loop (see [26] for the different parameter ranges and the list of singular cases). To demonstrate the results of sections 2 and 3, we consider here two regular cases: a) the tangent level set encircles the separatrix from outside, and b) the tangent level set is inside the separatrix, to the left of the left center point, see Figure 4. We show that in the former case the non-twist set remains empty whereas in the latter case there is an impacting non-twist torus (see Figure 6).

In fact, one can show that for any regular wall position of the first type (or, respectively, of the second type) the non-twist set remains empty (respectively, has at least one non-twist torus). Indeed, this follows from the fact that for the impact system, on the regular set, $\Theta(I) =$

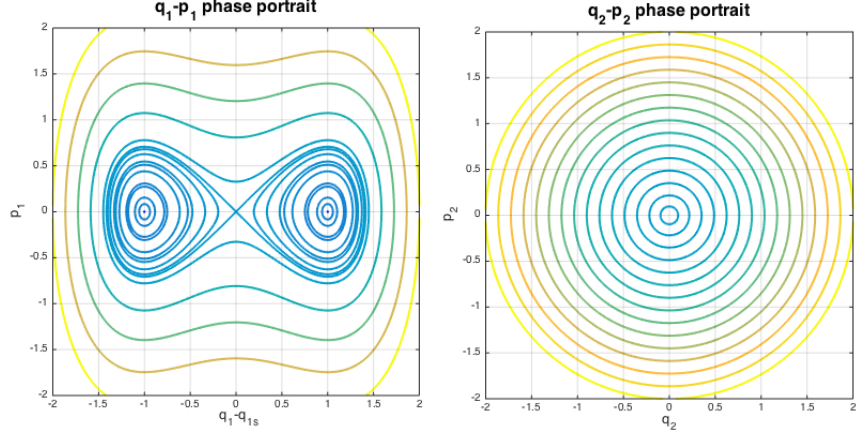


Figure 3: Energy level lines in the phase space (q_1, p_1) (left), (q_2, p_2) (right)

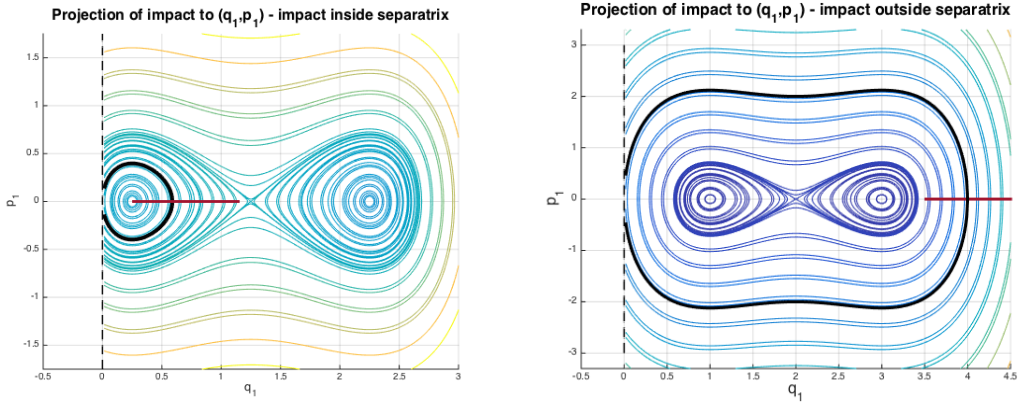


Figure 4: The separatrix and the wall locations. Here, $\lambda = 1$. The wall, located at $q_1^w = 0$, can be either inside (left, $q_{1s} = 1.25$) or outside (right, $q_{1s} = 2$) the separatrix. The tangent level line corresponding to J_{tan} is indicated in black. The cross-section Σ of the return map is depicted in crimson, and is defined on the impacting branch.

$\omega\tilde{T}_1(H - \omega I) = \omega T_1(H - \omega I) - \omega \Delta t_{travel}(H - \omega I)$, so $\Theta'(I) = -\omega^2(T_1'(H - \omega I) - \Delta t'_{travel}(H - \omega I))$. For $I = (H \pm \delta)/\omega$, the first term approaches $\pm 1/\delta$ as $\delta \rightarrow 0$ (there H_1 is in the δ neighborhood of the separatrix). However, for $I = (H - V_1(0) - \rho)/\omega$ (where H_1 is larger by ρ from the tangent energy leaf, $V_1(0)$), the second term approaches $1/\sqrt{\rho}$ as $\rho \rightarrow 0$. For regular wall position the tangent level set and the separatrix are bounded away from each other, and thus it follows that if the tangency occurs inside the separatrix ($V_1(0) < 0$) then, for sufficiently small δ, ρ , the rotation function derivative, $\Theta'(I)$, must change sign over the interval $I \in [(H + \delta)/\omega, (H - V_1(0) - \rho)/\omega] \subset S_g(H, \delta, \rho/\omega)$, and hence there exists at least one non-twist torus in the good set. On the other hand, if $V_1(0) > 0$ then $\Theta'(I) < 0$ for all $I < H/\omega$ and thus the non-twist set remains empty even with impact. See Figure 6 for illustration.

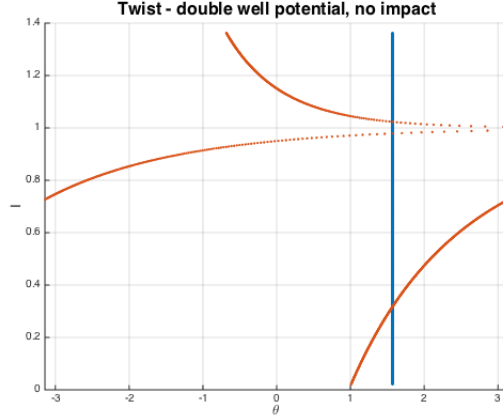


Figure 5: The twist in the system described by H_{int} , on the energy surface $H = 1$. In blue is a line of initial (I, θ) values, and in red - the corresponding $(I' = I, \theta')$ values following a single iteration of the integrable return map (wrapped in 2π). Here $I = 1$ corresponds to $H_1 = 0$. Due to the singularity at the separatrix, the twist changes direction between energies inside and outside the separatrix. In either case, there is no non-twist torus, due to the monotonicity of T_1 .

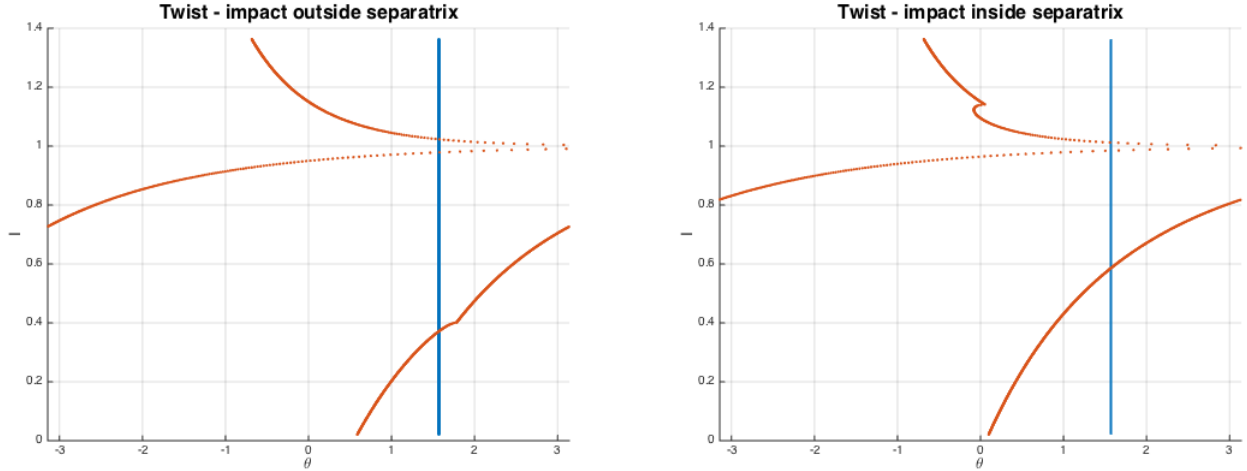


Figure 6: The twist in θ when impact is outside (left) or inside (right) of the separatrix. The points of non-smoothness correspond to I_{tan} , in which Δt_{travel} is continuous but not smooth. I values below this value correspond to impacting trajectories. As can be seen to the left, when the impact is outside the separatrix ($V_1(0) > 0$) the impact “contributes” to the same direction of the original, non-impacting twist. To the right, twist monotonicity is destroyed when impact is inside the separatrix ($V_1(0) < 0$) and a single non-twist torus is created at an intermediate point $I_{NT} \in (1, I_{tan})$.

Near integrability results

Figures 7-8 demonstrate numerically the near-integrability results described in section 3, and in particular the equivalence between the perpendicular and near perpendicular cases. Figure 7 depicts the dynamics of the return map in the (θ, I) plane. Examined are the cases of a near perpendicular, straight wall with an underlying integrable structure, a perpendicular wall with underlying near integrable structure, and the near perpendicular, near integrable combination. In all three cases, near integrable behavior in the form of KAM tori and resonances can be seen in the regions bounded away from tangency and the separatrix. Identification of these regions is made easily using the Impact Energy-Momentum Bifurcation Diagrams in Figure 8 (see below). For impacting trajectories the similarities between all three cases are evident. For non-impacting trajectories, integrable behavior is seen at the top figure ($\epsilon_w = 0.01$, $\epsilon_r = 0$) whereas, naturally, the remaining cases ($\epsilon_r \neq 0$) exhibit near integrable behavior even when the trajectories do not hit the wall¹.

In Figure 8, the same dynamics are depicted in the (H_{int}, I) plane, using an Impact Energy-Momentum Bifurcation Diagram, providing insights about the structure of the flow at different energy values; The classical Energy-Momentum Bifurcation Diagram (EMBD) [21, 2] for the smooth Hamiltonian is, in our case, a plot in the (H, I) space, where H is the energy of the integrable system and I is the action variable in the (q_2, p_2) phase space. In this plot the regions of allowed motion are shaded grey, and the curves corresponding to the (H_{int}, I) values on singular level sets of the system are depicted as dashed lines (respectively, solid lines) for singular level sets that include normally hyperbolic (respectively, normally elliptic) circles. Together with either Fomenko graphs or indicators of the number of Liouville leaves in each region [8, 2], such plots help to classify the dynamics on different energy surfaces.

Here we introduce a new variant to this representation, the Impact-EMBD, in which we add the projection of the conditions of impact (blue) and tangency (green) into the EMBD. When the wall is perpendicular, this projection results in a line which corresponds to tangent tori, and which separates between impacting and non-impacting trajectories. When the wall is not perpendicular, due to the breaking of the symmetry, the condition for tangency projects onto the I-EMBD as a 2-dimensional zone. While in the symmetric case each point on the tangency line corresponded to tori on which all initial conditions achieved tangency at first collision, in the non-symmetric case this is satisfied by only a finite (see [26]) number of points on each torus in the tangency zone. For the non-perpendicular wall the minimal energy for impact again coincides with the

¹Near the separatrix the map (14) is not well defined: the same (θ, I) values may correspond to two different sections in the (q_1, p_1) plane. One needs to use the separatrix map to obtain well defined sections there. Since the separatrix is not studied here, yet we want to present the global behavior, we do extend the marked section across the separatrix and ignore for now the observed artificial multiplicity which appears for trajectories that cross the separatrix.

minimal energy for a possible tangency. By projecting the dynamics into the I-EMBD we achieve a classification of the different types of trajectories in relation to the impact and internal phase space structure. These behaviors are then demonstrated in the (θ, I) plane (notice that the vertical axis in both projections corresponds to I values, which, together with fixing the total energy, allows for straightforward inference between the two different projections).

5 Discussion

Near integrability results for a class of 2 d.o.f separable mechanical impact systems with a single wall were derived. When the wall conserves the symmetry of the integrable system - here, the separability - the system remains integrable. In particular, local sections allow to define Poincaré return maps that are smooth and satisfy the twist condition. We proved that breaking the separability of the system by the addition of a small regular perturbation, a small perturbation of the wall, making the wall soft, or a combination of all these effects together, may destroy the integrability of the return map, yet the map remains near integrable for a large portion of the phase space (Theorems 3.1, 3.5 and 3.7). For the case of a small regular perturbation and a slightly tilted, straight wall, an explicit form of the first order term in the perturbed return map was derived, a form which applies also to the soft impact formulation in the limit of very steep potential. The correction terms which arise from the steep potential part could be possibly derived as well (see [27]).

The dynamics near singularities of the impact system - separatrices and tangencies - are yet to be explored, as is the limit of large energy values. Away from tangency, the dynamics near the separatrix are expected to exhibit the usual separatrix splitting and homoclinic chaos, similar to the smooth case. The near tangent dynamics are expected to produce more exotic behavior, as is demonstrated in Figure 9. Notably, some aspects of this behavior have been explored by Neishtadt in [12], for a 1.5 d.o.f system with slow-fast dynamics. The system (1) may be reduced to such a system when $\omega_1(J) \gg \omega_2(I)$; Indeed, let us denote $\frac{T_1(J)}{T_2(I)} = \delta$, where $\delta > 0$ and small, define the slow time variable $\tau = \delta t$ and symbolically denote the slow variables

$$q_2 = q_2(\tau), \quad p_2 = p_2(\tau) \tag{34}$$

Since $q_1^w = \epsilon_w Q(q_2^w)$ the collision point with the wall varies slowly with the evolution of q_2 - $q_1^* = \epsilon_w Q(q_2^*(\tau))$. Similarly, the perturbation $\epsilon_r V_r(q_1, q_2)$ changes slowly in time - $\epsilon_r V_r(q_1; \tau)$. The slow-fast system can therefore be effectively reduced to a 1.5 degrees of freedom system with a slowly varying potential and a slowly moving wall, and the results of [12] can be applied. We leave for future works the relation of these results and the fascinating patterns seen in Figure 9.

Appendices

A Boundedness of the perturbation terms on the energy surface

Lemma A.1. *The perturbed energy surface corresponding to a constant energy level set $h = H_{int} + \epsilon_r V_r$ is bounded.*

Proof. This is a result of the assumptions on the potential form and the implicit function theorem. Note that since the system in consideration is mechanical, i.e. $H = \sum_{i=1,2} \frac{p_i^2}{2} + V_i(q_i) + \epsilon_r V_r(q_1, q_2)$, it is enough to show that the Hill region - the allowed region of motion in the configuration space, (q_1, q_2) - is bounded. Indeed, if the motion in q_1, q_2 is restricted to a compact Hill region, then from the assumptions on smoothness and boundedness the potential values V_1, V_2, V_r are bounded and thus so are the momenta, hence the energy surface is bounded.

Consider therefore the boundaries in q . These boundaries are the potential level sets which define the Hill region, and are defined by the equation $V_{int}(q_1, q_2) + \epsilon_r V_r(q_1, q_2) - h \equiv F(q_1, q_2; \epsilon_r) = 0$. For $\epsilon_r = 0$, by the S3B assumption, the solution of the equation $F(q_1^0, q_2^0; 0) = 0$ is a bounded region, i.e. there exists R such that $\|(q_1^0, q_2^0)\| < R(h)$ for all (q_1^0, q_2^0) on the energy surface $H_{int} = h$. Consider first energy levels which are bounded away from those containing fixed points of the integrable system (by the S3B assumption there are a finite number of such excluded energy intervals). Now, for $F(q_1^\epsilon, q_2^\epsilon; \epsilon) = 0$, since $\|\nabla V_{int}\| > const. > 0$ on such surfaces, by the implicit function theorem there exists ϵ_0 such that for all $\epsilon < \epsilon_0$, there exist solutions $(q_1^\epsilon, q_2^\epsilon)$ which are ϵ -close to (q_1^0, q_2^0) , and hence, for example, for sufficiently small ϵ_0 , $\|(q_1^\epsilon, q_2^\epsilon)\| < 2R(h)$. Hence, q_1, q_2 are bounded and the Hill region is indeed compact.

Now consider the intervals of energy which contain points that are close to the extremal points of the potential (the fixed points of the Hamiltonian system), i.e. where $\|\nabla V_{int}\| = 0$. The number of these points is finite and they are contained in a bounded domain, from the assumed structure of the integrable Hamiltonian. Furthermore, as the Hill regions S_{h_1}, S_{h_2} for different energy values $h_1 < h_2$ are level sets of the potential function, these are nested regions in the configuration space - $S_{h_1} \subset S_{h_2}$. Hence the energy surfaces corresponding to singular energy level sets and their nearby energy surfaces are bounded as well. \square

B Conditions I-V for the soft impact system

Theorem 1 in [17] establishes that finite segments of trajectories of the smooth impact Hamiltonian flow

$$H(q, p) = \frac{p^2}{2} + U(q) + V(q; \epsilon_b), \quad (35)$$

with energy $H < H_{max}$ limit to those of the hard impact system in some general bounded domain D in \mathbb{R}^d or \mathbb{T}^d , in the C^r topology, provided these segments contain only regular reflections, and the potentials satisfy some general conditions; The potential $V(q; \epsilon_b)$ is assumed to be a soft-billiard potential (satisfying conditions I-IV of [17, 27], which are also listed below). The smooth, C^{r+1} , potential U is quite general - one only assumes that on the domain boundary, which is assumed to be of finite length, U is bounded from below by $\hat{U} > -\mathcal{E}$ (condition V in [17], see below), where \mathcal{E} denotes the limit of the billiard potential energy at the wall ($V(q; \epsilon_b)$ as $q \rightarrow q^w$ and $\epsilon_b \rightarrow 0$, so \mathcal{E} may be finite, similar to the example in Eq. (33) or infinite as in Eq. (32)). Finally, setting the maximal energy to $H_{max} < \mathcal{E} + \hat{U}$ insures that particles with $H < H_{max}$ do not escape from the billiard domain. Here, we denote the form of the soft impact potential by $b \cdot V_b(\cdot, \epsilon_b)$ and adopt the convention that the barrier height $\mathcal{E} \geq b$ and can, again, be either finite or infinite.

To apply the above result to the current work we need to address only one issue - formally, for simplicity, the conditions in [17] were stated for compact domains D with finite length boundary ∂D , whereas here the domain $D = \{(q_1, q_2) | q_1 \geq q_1^w = \epsilon_w Q^w(q_2), q_2 \in \mathbb{R}\}$ is unbounded and has infinite length boundary $\partial D = \{(q_1^w(q_2), q_2), q_2 \in \mathbb{R}\}$. Noting that for finite energies H , by the S3B assumption on V_{int} and V_r , the Hill regions for all $H \leq H_{max}$ are compact and are contained in the compact Hill region of H_{max} (see appendix A), solves this formal problem; In particular, one can choose

$$\hat{V} = \min_{q \in D_{Hill}(H_{max})} V_{int}(q) - 1 \leq \min_{q \in D_{Hill}(H_{max})} (V_{int}(q) + \epsilon_r V_r(q, \epsilon_r)) \quad (36)$$

and the results of [17] directly apply as long as the potential $V_b(\cdot, \epsilon_b)$ of (31) is a billiard-like-potential on D (satisfies the conditions I-IV that are listed below on this domain, with the billiard boundary set at $q_1 = q_1^w$). In fact, it is sufficient to require that these conditions are satisfied on $D \cap D_{Hill}(H_{max})$.

The conditions I-V of [17] are listed below, almost verbatim: in some places notation is adjusted and simplified to the setting of the current paper, which is two-dimensional and has only one boundary component with no corners. Additionally, some remarks regarding the current setup are included.

Condition I. For any fixed compact region $K \subset D$, the potential $V_b(q_1, q_2; \epsilon_w; \epsilon_b)$ diminishes

along with all its derivatives as $\epsilon_b \rightarrow 0$:

$$\lim_{\epsilon_b \rightarrow 0} \|V_b(q_1, q_2; \epsilon_w; \epsilon_b) |_{(q_1, q_2) \in K}\|_{C^{r+1}} = 0$$

We assume that the level sets of V_b may be realized by some finite function near the boundary. Let N denote the fixed (independent of ϵ_b) neighborhood of the billiard boundary ∂D (for example, here, $N = \{q | q_1^w < q_1 < 0.1\}$). Assume that for all small $\epsilon_b \geq 0$ there exists a *pattern function*

$$Q(q_1, q_2; \epsilon_b) : N \rightarrow \mathbb{R}^1,$$

which is C^{r+1} with respect to (q_1, q_2) in N and depends continuously on ϵ_b (in the C^{r+1} topology, so it has, along with all its derivatives, a proper limit as $\epsilon_b \rightarrow 0$).

Further assume that the following is fulfilled:

Condition IIa. The billiard boundary is a level surface of $Q(q_1, q_2; 0)$:

$$Q(q_1, q_2; \epsilon_b = 0) |_{(q_1, q_2) \in \partial D} \equiv \mathcal{Q} = \text{const.}$$

In the neighborhood N of the barrier ∂D (so $Q(q_1, q_2; \epsilon_b = 0)$ is close to \mathcal{Q}), define a *barrier function* $W(Q; \epsilon_b)$, which is C^{r+1} smooth in Q , is continuous in ϵ_b , and does not depend explicitly on (q_1, q_2) . Also assume that there exists ϵ_0 such that conditions IIb-c are satisfied.

Condition IIb. For all $\epsilon_b \in (0, \epsilon_0]$ the potential level sets in N are identical to the pattern function level sets, and thus

$$b \cdot V_b(q_1, q_2; \epsilon_b) |_{(q_1, q_2) \in N} \equiv W(Q(q_1, q_2; \epsilon_b) - \mathcal{Q}; \epsilon_b).$$

Condition IIc. For all $\epsilon_b \in (0, \epsilon_0]$, ∇V_b does not vanish in the finite neighborhood of the boundary surface N ; thus

$$\nabla Q |_{(q_1, q_2) \in N} \neq 0,$$

and for all $Q(q_1, q_2; \epsilon_b) |_{(q_1, q_2) \in N}$,

$$\frac{d}{dQ} W(Q - \mathcal{Q}; \epsilon_b) \neq 0.$$

Adopt the convention that $Q > \mathcal{Q}$ corresponds to the points near ∂D inside the billiard.

Condition III. There exists a constant $\mathcal{E} > 0$ (\mathcal{E} may be infinite) such that as $\epsilon_b \rightarrow +0$ the

barrier function increases from zero to \mathcal{E} across the boundary ∂D :

$$\lim_{\epsilon_b \rightarrow +0} W(Q; \epsilon_b) = \begin{cases} 0, & Q > \mathcal{Q} \\ \mathcal{E}, & Q < \mathcal{Q} \end{cases}$$

Condition IV. As $\epsilon_b \rightarrow +0$, for any fixed W_1 and W_2 such that $0 < W_1 < W_2 < c$, the function $Q(W; \epsilon_b)$ tends to zero uniformly on the interval $[W_1, W_2]$ along with all of its $(r + 1)$ derivatives.

For example, one can take here $Q(q_1, q_2; \epsilon_w) = q_1 - \epsilon_w Q^w(q_2)$, and billiard-like potential functions of the form $b \cdot V_b = W(Q(q; \epsilon_w), \epsilon_b)$, with $W(Q, \epsilon_b) = b \cdot \exp(-Q/\epsilon_b)$ and $W(Q, \epsilon_b) = -b \cdot \epsilon_b/Q$ corresponding to the billiard potential (32),(33) respectively, and $\mathcal{E} \geq b$. According to Theorem 1 of [17], we can choose ϵ_w to depend on ϵ_b or take them independent.

The last condition is concerned with the addition of the smooth component of the potential $U(q)$ assuring that together with the billiard-like potential, particles that are initially in D cannot escape. Defining $\hat{U} = \min_{q \in \partial D} U(q)$ one assumes that:

Condition V. $U(q)$ is a C^{r+1} smooth potential bounded in the C^{r+1} topology on an open set \mathcal{D} , where $\bar{D} \in \mathcal{D}$. The minimum of U on the boundary ∂D satisfies $\hat{U} > -\mathcal{E}$.

Using in the above definition $U(q) = V_{int}(q) + \epsilon_r V_r(q)$ it suffices in our setting to require $\hat{U} > -b$. In particular, Theorem 1 of [17] then applies to trajectory segments with bounded energies which satisfy $H < H_{max}(b) = b + \hat{V} = b + \min_{q \in D_{Hill}(H_{max})} V_{int} - 1$ where b is the minimal billiard potential barrier height.

References

- [1] V.I. Arnold. *Mathematical Methods of Classical Mechanics*, volume 60. Springer Science & Business Media, 2013.
- [2] V.I. Arnold, V.V. Kozlov, and A.I. Neishtadt. *Mathematical Aspects of Classical and Celestial Mechanics*, volume 3. Springer Science & Business Media, 2007.
- [3] A.V. Artemyev and A.I. Neishtadt. Violation of adiabaticity in magnetic billiards due to separatrix crossings. *Chaos: An Interdisciplinary Journal of Nonlinear Science*, 25(8):083109, 2015.
- [4] N. Berglund. Billiards in a potential: variational methods, periodic orbits and KAM tori. 1996.

- [5] N. Berglund. Classical billiards in a magnetic field and a potential. *Nonlinear Phenomena in Complex Systems*, 3(1):61–70, 2000.
- [6] N. Berglund and H. Kunz. Integrability and ergodicity of classical billiards in a magnetic field. *Journal of statistical physics*, 83(1-2):81–126, 1996.
- [7] M. Bernardo, C. Budd, A.R. Champneys, and P. Kowalczyk. *Piecewise-smooth dynamical systems: theory and applications*, volume 163. Springer Science & Business Media, 2008.
- [8] A.V. Bolsinov and A.T. Fomenko. *Integrable Hamiltonian systems: Geometry, Topology, Classification*. CRC Press, 2004.
- [9] N. Chernov and R. Markarian. *Chaotic Billiards*. Number 127. American Mathematical Soc., 2006.
- [10] R. de la Llave. A tutorial on KAM theory. In *Proceedings of Symposia in Pure Mathematics*, volume 69, pages 175–296. Providence, RI; American Mathematical Society; 1998, 2001.
- [11] H. Dullin. Linear stability in billiards with potential. *Nonlinearity*, 11(1):151, 1998.
- [12] I. Gorelyshev and A. Neishtadt. Jump in adiabatic invariant at a transition between modes of motion for systems with impacts. *Nonlinearity*, 21(4):661, 2008.
- [13] I.V. Gorelyshev and A.I. Neishtadt. On the adiabatic perturbation theory for systems with impacts. *Journal of applied mathematics and mechanics*, 70(1):4–17, 2006.
- [14] A. Granados, S.J. Hogan, and T.M. Seara. The scattering map in two coupled piecewise-smooth systems, with numerical application to rocking blocks. *Physica D*, 269:1–20, 2014.
- [15] G. Haller. *Chaos Near Resonance*, volume 138. Springer Science & Business Media, 2012.
- [16] A. Kazakov, N. Kulagin, and L. Lerman. Dynamical features in a slow-fast piecewise linear Hamiltonian system. *Mathematical Modelling of Natural Phenomena*, 8(5):155–172, 2013.
- [17] M. Kloc and V. Rom-Kedar. Smooth Hamiltonian systems with soft impacts. *SIAM Journal on Applied Dynamical Systems*, 13(3):1033–1059, 2014.
- [18] V.V. Kozlov and D.V. Treshchëv. *Billiards: a genetic introduction to the dynamics of systems with impacts*, volume 89. American Mathematical Soc., 1991.
- [19] M. Kunze, T. Kupper, and J. You. On the application of KAM theory to discontinuous dynamical systems. *Journal of Differential Equations*, 139(1):1–21, 1997.

- [20] L. Lerman and V. Rom-Kedar. A saddle in a corner—a model of collinear triatomic chemical reactions. *SIAM Journal on Applied Dynamical Systems*, 11(1):416–446, 2012.
- [21] L.M. Lerman and Ya.L. Umanski. *Four Dimensional Integrable Hamiltonian Systems with Simple Singular Points*, *Transl. Math. Monographs*, 1998.
- [22] O. Makarenkov and J.S.W. Lamb. Dynamics and bifurcations of nonsmooth systems: A survey. *Physica D: Nonlinear Phenomena*, 241(22):1826–1844, 2012.
- [23] J.D. Meiss. *Differential Dynamical Systems*, volume 14. Siam, 2007.
- [24] K. Meyer, G. Hall, and D. Offin. *Introduction to Hamiltonian Dynamical Systems and the N-Body Problem*, volume 90. Springer Science & Business Media, 2008.
- [25] A.I. Neishtadt and A.V. Artemyev. Destruction of adiabatic invariance for billiards in a strong nonuniform magnetic field. *Physical review letters*, 108(6):064102, 2012.
- [26] M. Pnueli. Dynamics in a Hamiltonian impact system. Master’s thesis, Weizmann Institute of Science, 2016.
- [27] A. Rapoport, V. Rom-Kedar, and D. Turaev. Approximating multi-dimensional Hamiltonian flows by billiards. *Communications in mathematical physics*, 272(3):567–600, 2007.
- [28] A. Rapoport, V. Rom-Kedar, and D. Turaev. Stability in high dimensional steep repelling potentials. *Communications in Mathematical Physics*, 279(2):497–534, 2008.
- [29] M. Robnik and M.V. Berry. Classical billiards in magnetic fields. *Journal of Physics A: Mathematical and General*, 18(9):1361, 1985.
- [30] V. Rom-Kedar and D. Turaev. Billiards: A singular perturbation limit of smooth Hamiltonian flows. *Chaos: An Interdisciplinary Journal of Nonlinear Science*, 22(2):026102, 2012.
- [31] V. Zharnitsky. Invariant tori in Hamiltonian systems with impacts. *Communications in Mathematical Physics*, 211(2):289–302, 2000.

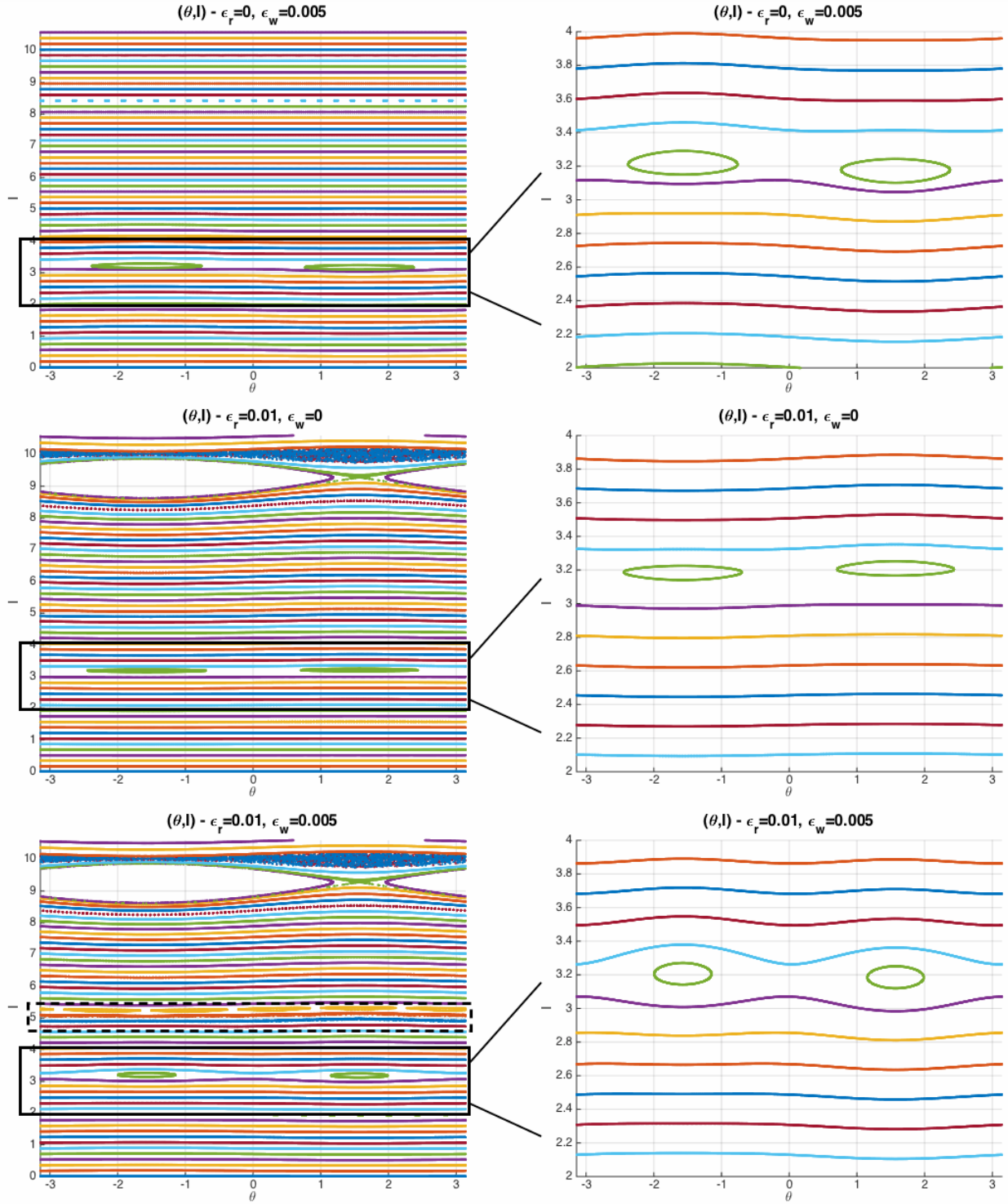


Figure 7: Poincaré return map (θ', I') for the following cases: (top) $q_1^w = \epsilon_w q_2^w, \epsilon_w = 0.01, \epsilon_r = 0$; (middle) $\epsilon_w = 0, \epsilon_r = 0.005$; (bottom) $q_1^w = \epsilon_w q_2^w, \epsilon_w = 0.01, \epsilon_r = 0.005$. Initial conditions for all three figures are the same. To the left, the entire possible range of I values is depicted. To the right, a zoom on a region away from the separatrix and from tangency is shown. KAM tori and resonances can be seen, as well as the similarity between the three different settings. The distinction between impacting and non-impacting I values can be easily made by comparison with Figure 8.

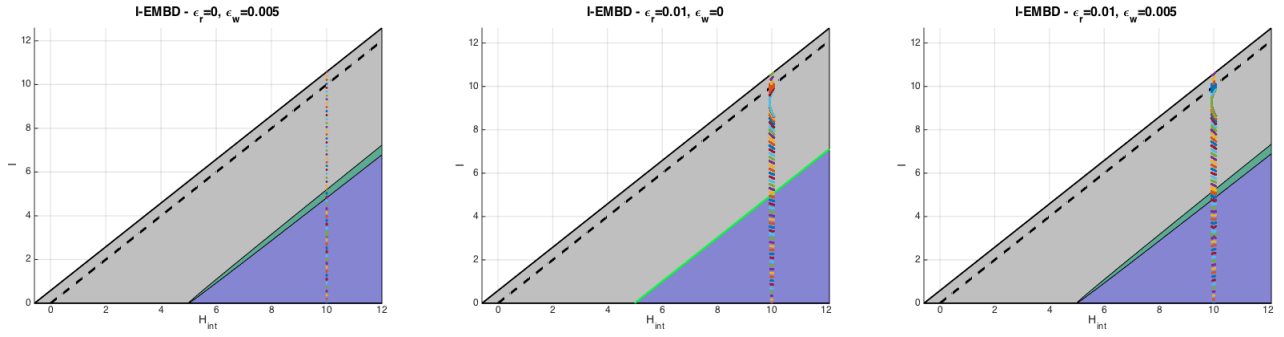


Figure 8: I-EMBD (H_{int}, I) for the following cases: (left) $q_1^w = \epsilon_w q_2^w, \epsilon_w = 0.01, \epsilon_r = 0$; (middle) $\epsilon_w = 0, \epsilon_r = 0.005$; (right) $q_1^w = \epsilon_w q_2^w, \epsilon_w = 0.01, \epsilon_r = 0.005$. Notice that in the cases of a small tilt (left and right), tangency is projected as a zone, whereas for the vertical wall it is projected as a line. The return map values depicted in Figure 7 are projected here into the I-EMBD.

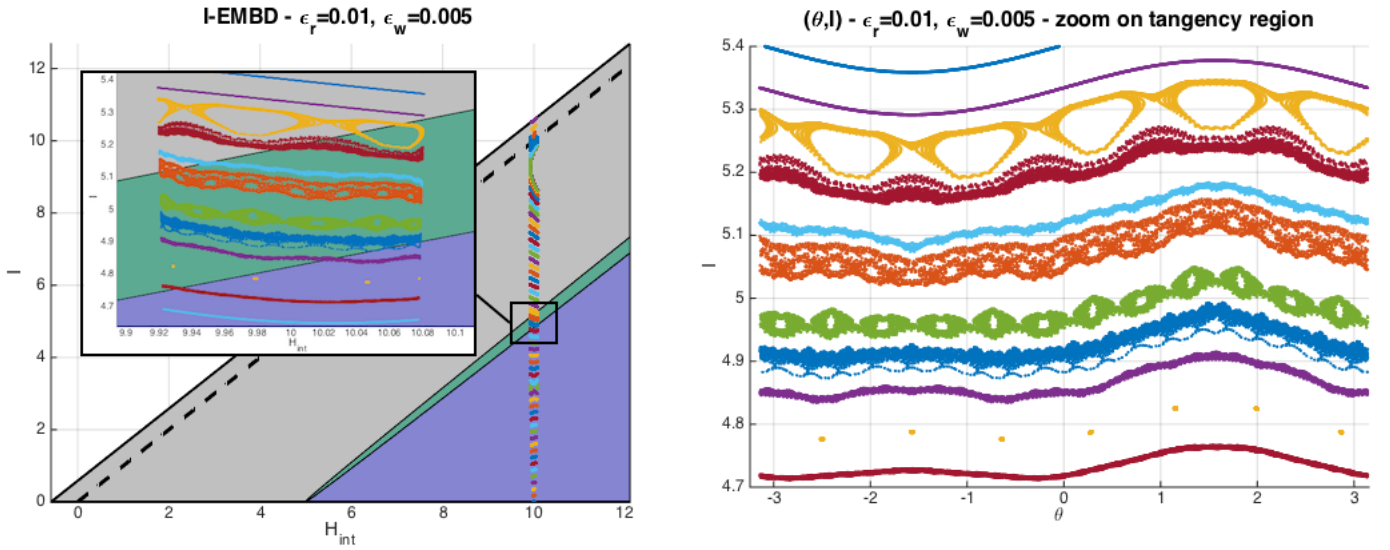


Figure 9: I-EMBD (right) and return map values (left) for near tangent initial conditions, indicated in the bottom left image in Figure 7 by a dashed rectangle (higher resolution of initial values is applied to the relevant region).